High Speed Forming of the Light-Weight Wrought Alloys

E. El-Magd, M. Abouridouane

Department of Materials Science (LFW), Aachen University, Germany

Abstract

The deformation and fracture behaviour of the Al-alloy AA7075, Mg-alloy AZ80, and Ti-alloy Ti-6Al-4V were investigated in quasi-static and dynamic uniaxial compression and tension tests at strain rates in the range of 0.001 $s^{-1} \leq \dot{\varepsilon} \leq 5000\ s^{-1}$ and temperatures between 20°C and 500°C. Shear tests with hat shaped specimens of AZ80 were carried out by quasi-static and dynamic loading in the shear rate range of $0.01\,\mathrm{s}^{-1} \leq \dot{\gamma} \leq 116000\,\mathrm{s}^{-1}$ *at a temperature of 20°C.*

For strain rates of $\dot{\varepsilon} \leq 10\ s^{-1}$, the tests were carried out using a computer numerical controlled hydraulic testing machine. High strain rate experiments with $\dot{\varepsilon} \geq 1000\ s^{-1}$ were performed on a Split Hopkinson Pressure Bar. Using the experimentally determined flow curves, the effect of strain rate and temperature on the compressive deformation at fracture was determined, showing that the forces required for forming as well as the limits of the possible deformation are controlled by strain rate und temperature. Under dynamic loading, both AA7075 and AZ80 show an increase of the deformation degree at fracture with increasing strain rate, whereas the Ti-6Al-4V shows a decrease of it. The investigated mechanical material behaviour (strain hardening, strain rate sensitivity, and thermal softening) and metallographic investigations of the deformed specimens in dynamic compression tests allow an explanation for character, formation, and evolution of damage in the deformed material. Constitutive material laws, whose parameters are determined from the experimental data, can be applied to describe the influence of strain rate and temperature on the mechanical material behaviour in compression, tension and shear tests. These material laws are to be implemented into the FE simulation, in order to determine the local state of stress and strain at time of the fracture. Through combination of experiment and simulation, a failure criterion for ductile fracture could be determined for AA7075 under quasi-static and dynamic tensile loading.

Keywords:

Flow behaviour, High strain rates, Constitutive material law

1 Introduction

Forming and machining of brittle materials such as Magnesium alloys with conventional methods is limited, so that an intermediate treatment of the work piece should be necessary. Under dynamic loading, metallic materials exhibit an increase of flow stress and ductility with increasing deformation rate [1]. Consequently, materials of lower ductility can be deformed to higher strains using high strain rate deformation processes such as magnetic or explosive forming [2]. Therefore, adequate knowledge is needed. Furthermore, constitutive material laws are necessary to describe the material behaviour in simulation of high strain rate deformation processes as crash test and high speed cutting.

The strain rate and temperature considerably influence the material flow behaviour in deformation processes. Under quasi-static loading, strain hardening causes an increase of force and acts stabilising on the deformation process. In case of dynamic loading, additional influences on the flow stress and the ductility of the material have to be taken into consideration. With increasing deformation rate, the strain rate sensitivity increases, leading to a higher local value of flow stress and stabilises the deformation. On the other hand, the adiabatic character of the deformation process reduces the flow stress and promotes instability. Furthermore, the deformation process is influenced by inertia [3] and mechanical wave propagation effects [4]. The aim of this work is to characterise, model, and simulate the mechanical material behaviour of the light-weight wrought alloys, AA7075, AZ80, and TiAl6V4 subjected to high strain rates compression, tension, and shear loading.

2 Experimental results

Quasi-static and dynamic compression tests were carried out on cylindrical specimens of Al-alloy AA7075 in the T7351 condition as well as Mg-alloy AZ80 and Ti-alloy Ti-6Al-4V in the as extruded condition. The tests were conducted at strain rates in the range of $0{,}001\ s^{-1} \leq \dot{\varepsilon} \leq 5000\ s^{-1}$ and temperatures between $20\ °C \leq \vartheta \leq 500\ °C$. Experimentally determined flow curves of the investigated materials are represented in Figure 1. The stress of the quasi-static flow curves increases continuously with increasing strain due to strain hardening. With higher strain rates $\dot{\varepsilon} \geq 1000\ s^{-1}$, the flow curves show an increase of flow stress at lower strains, on the other hand a decrease of stress beyond a stress maximum due to thermal softening caused by the adiabatic character of the deformation process resulting in a temperature increase in the specimen at high strains. Under dynamic loading, both AA7075 and AZ80 show an increase of the deformation at fracture with increasing strain rate, whereas the Ti-6Al-4V shows a decrease of it. Furthermore, the higher the temperature the lower the 0.2% proof stress and the higher the ductility of the tested materials.

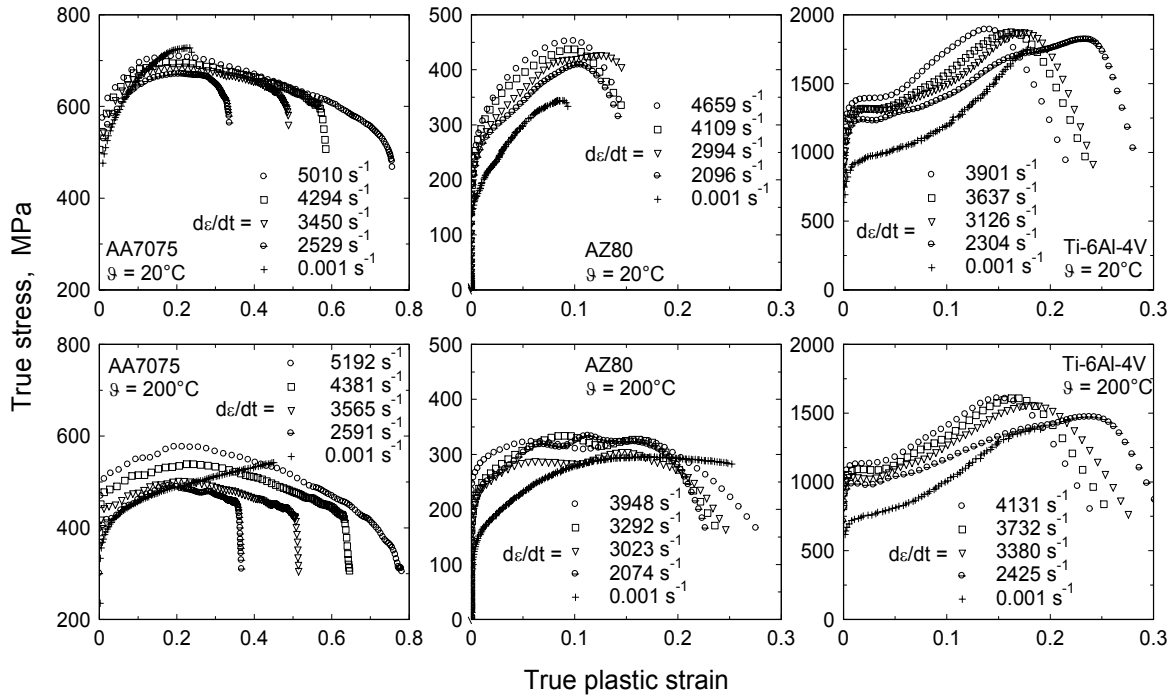

***Figure 1**: Flow curves of AA7075, AZ80 and Ti-6Al-4V from compression tests at different stain rates and temperatures*

The experimental results of the tensile and shear tests at room temperature on AA7075 and AZ80 respectively are illustrated in Figure 2. In both cases the influence of the strain rate on the flow stress and deformation at fracture is obvious. Under dynamic loading, the stress-strain curves show a maximum at lower strains due to contrary effects of the strain rate sensitivity and thermal softening on the stress. Furthermore, the ductility of the tested alloys is controlled by these effects.

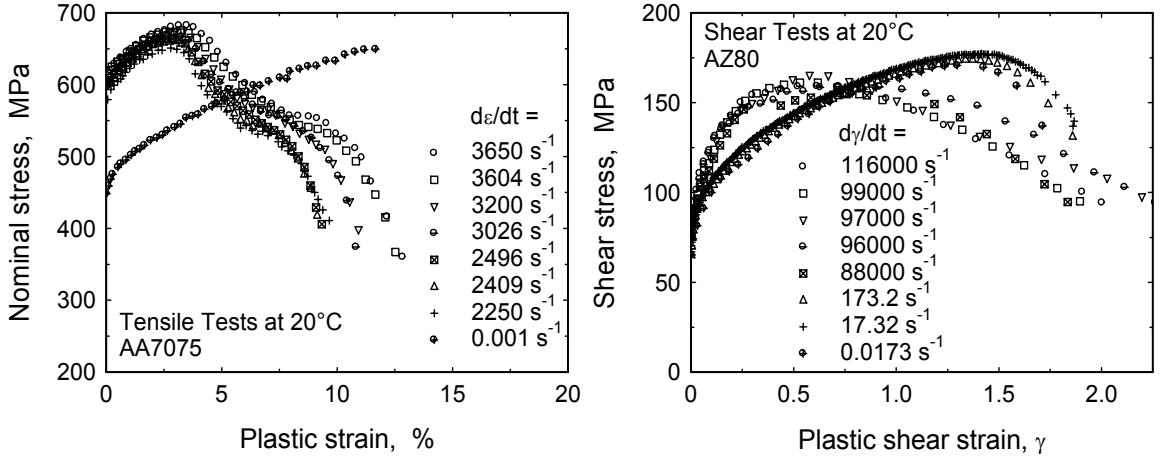

***Figure 2:** Stress-strain curves of AA7075 in tension and of AZ80 in shear tests at different strain rate and 20°C*

2.1 Effect of strain rate and temperature on deformation degree at fracture

The deformation degree at fracture, defined as the relative reduction of the height $(-\Delta H / H_0)f$ of the cylindrical compression specimen at fracture, is considered as a measure for the compressive ductility of the material. The deformation degree at fracture was determined as a function of the strain rate for different temperatures as represented in Figure 3. At room temperature with increasing strain rate in the range of $0{,}001\ s^{-1} \leq \dot{\varepsilon} \leq 1\ s^{-1}$, the deformation degree at fracture shows an increase due to the stabilising effect of the strain rate sensitivity for all tested materials. Under impact loading with strain rates higher than $1000\ s^{-1}$, the ductility of AA7075 and AZ80 increases sharply with the strain rates due to higher strain rate sensitivity, while it decreases for Ti-6Al-4V because of the dominating influence of strain rate on the damage process. Under quasi-static loading with $\dot{\varepsilon} = 0{,}001\ s^{-1}$, the fracture strain increases with the temperature. No fracture was detected at temperatures of 150°C, 200°C, 450°C and higher for AA7075, AZ80, and Ti-6Al-4V respectively up to values of $(-\Delta H / H_0) = 80\%$. In case of dynamic loading the ductility of AZ80 and Ti-6Al-4V were clearly influenced by temperature, while AA7075 shows a little temperature dependence.

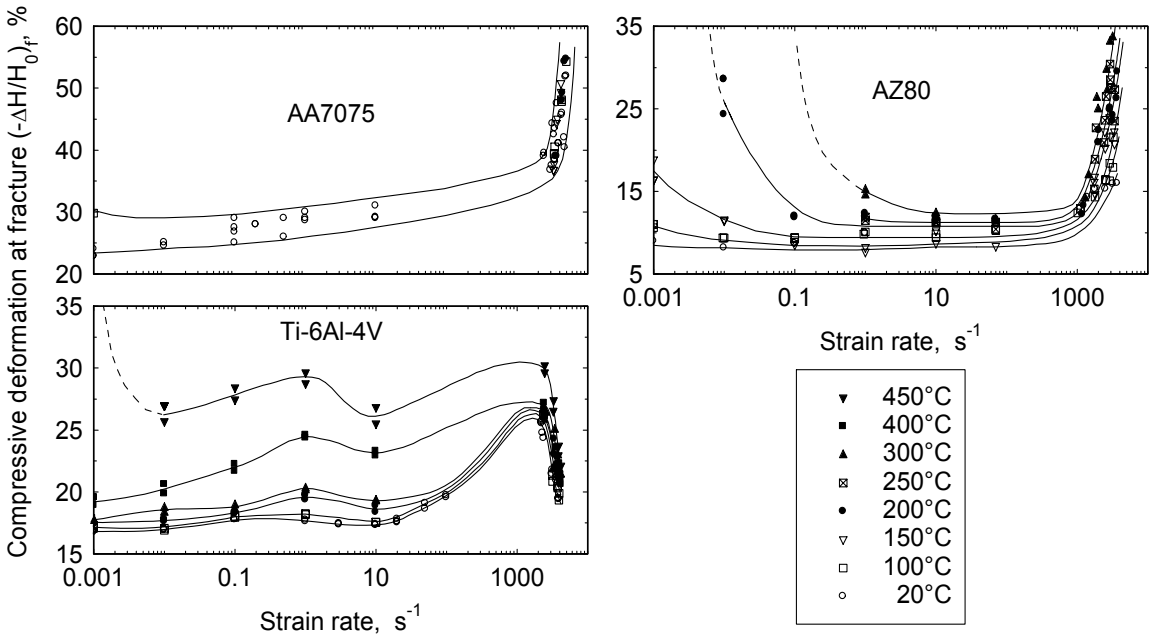

***Figure 3**: Deformation degree at fracture as a function of the strain rate and temperature (AA7075, AZ80 and Ti-6Al-4V)*

2.2 Damage by dynamic adiabatic shear bands

In order to examine the failure behaviour of the tested materials, metallographic investigations were accomplished on compressed specimens from AA7075 at test conditions $\dot{\varepsilon} = 4000\ s^{-1}$, $\vartheta = 20°C$ up to a pre-defined deformation $(-\Delta H/H_0) = 50\%$ for both of AZ80 and Ti-6Al-4V at $\dot{\varepsilon} = 2000\ s^{-1}$, $\vartheta = 20°C$ and $(-\Delta H/H_0) = 18\%$. Longitudinal sections of the impacted specimens are represented in Figure 4. The deformed specimens come to ductile shear fracture which localised along the surface of the compression cone. Compression cone usually causes by the friction between the sample and upsetting bars. This effect of friction increases in dynamic compression tests due to wave reflection from the output bar. The damage initiates from the contact surfaces where the friction constrains

the radial deformation of the specimen. A higher magnification of the longitudinal section in AA7075 and Ti-6Al-4V shows a creation of shear bands. In case of AZ80, the deformation localisation was detected along the compression cone, but has not led to shear band formation.

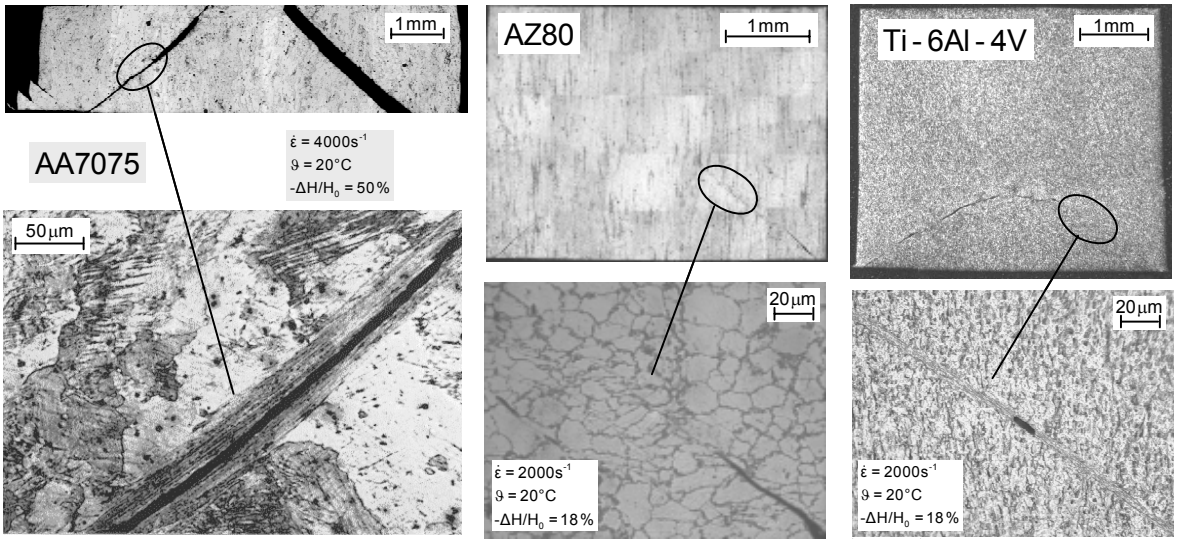

Figure 4: *Deformation localization and damage within specimens of AA7075, AZ80 and Ti-6Al-4V, deformed under impact loading at room temperature*

3 Constitutive modelling for material flow curves

3.1 Material law for impact loading

In case of dynamic loading with strain rates higher than 1000 s^{-1}, the influence of the strain rate can be represented by a linear relation $\sigma = \sigma + \eta\dot{\varepsilon}$ according to the damping mechanism as it was confirmed e.g. in [5]. The parameter σ_h signifies the stress extrapolated from the range of high strain rates down to $\dot{\varepsilon} = 0\,s^{-1}$; η is the damping parameter. The influence of the temperature increase on the flow stress can be considered by a multiplicative function, so that the material behaviour can be described by [6]:

$$\sigma = \left[K(B+\varepsilon)^n + \eta\dot{\varepsilon}\right] exp\left[-\beta\frac{T-T_0}{T_m}\right] \tag{1}$$

where *B*, *K*, and n are material constants. T_m, T_0, and *T* are the absolute melting point, room temperature, and actual temperature respectively. *β* is a material constant which can be set to 3 for several materials [6]. Assuming that the major part of deformation energy is transferred to heat during a dynamic deformation process and that the remaining part is consumed by an internal energy increase e.g. due to dislocation multiplication. The temperature increase can be determined by $\bar{\rho}\,\bar{c}\,dT = \kappa\,\sigma\,d\varepsilon$. In this equation $\kappa = 0.9$ [7] represents the fraction of energy transferred to heat, *ρ* and *c* are the density and the specific heat capacity of the material. With the relation between flow stress and temperature according to Equation (1), the increase of temperature can be determined as a function of strain by integration. The stress-strain relation under consideration of the two contrary influences of strain rate sensitivity and thermal softening results from the substitution of temperature in Equation (1):

$$\sigma = \frac{K(B+\varepsilon)^n + \eta\dot{\varepsilon}}{exp\left[\beta(T_S - T_0)/T_m\right] + a\int\left[K(B+\varepsilon)^n + \eta\dot{\varepsilon}\right]\dot{\varepsilon}dt} \tag{2}$$

with T_S is the test start temperature and $a = \kappa\beta/(T_m\overline{\rho c})$.

Figure 5 shows a comparison between computational results following Equation (2) (continuous curves) and experimental results from dynamic compression tests (markers) for AA7075-T7351, AZ80, and Ti-6Al-4V at different strain rates and 20°C. The parameters determined for AA7075 and AZ80 are given in Figure 5. In the case of the Ti-alloy, Equation (2) do not well describe the flow curves in the range of small strains $\varepsilon < 0.04$. In this range, the flow stress is approximately constant and equal to the 0.2% proof stress given by $R_{p0,2}$=1026 + 0.092 $\dot{\varepsilon}$ where $R_{p0,2}$ in MPa and $\dot{\varepsilon}$ in s^{-1}. If the stress value calculated by Equation (2) is less than $R_{p0,2}$ it is to be replaced by this value.

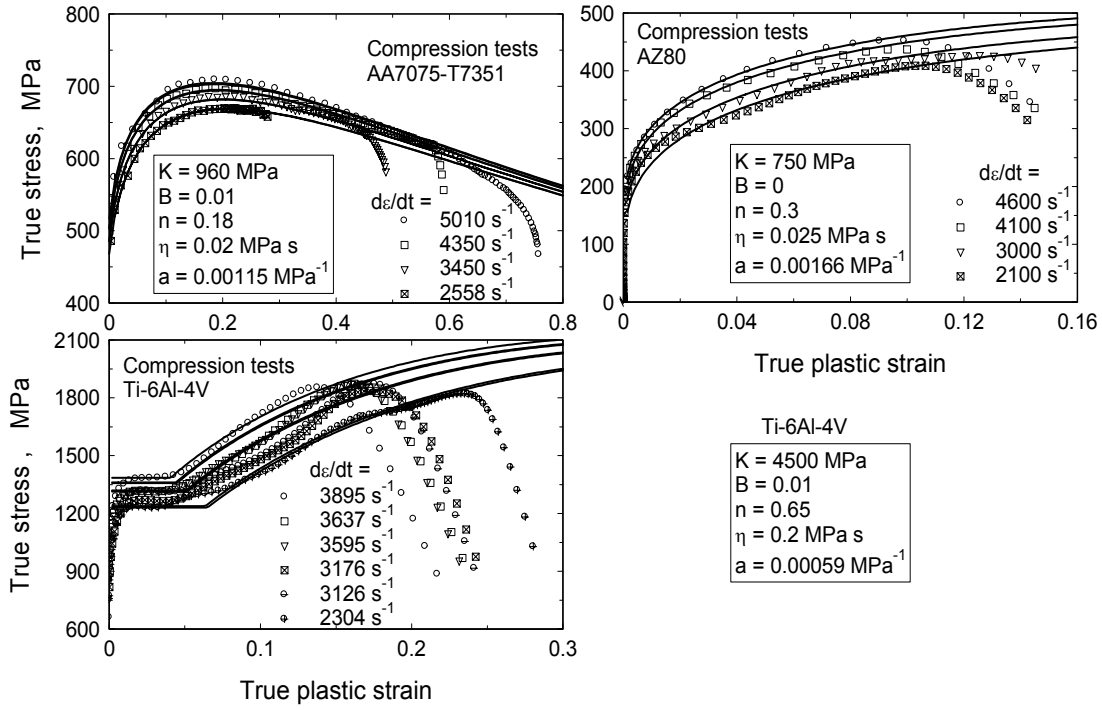

Figure 5: *Experimental and computational results of dynamic compression tests for AA7075, AZ80 and Ti-6Al-4V*

3.2 Material law for the whole range of strain rate and temperature

If the material behaviour is to be described in a larger range of strain rate and temperature, different physical influences must be combined. At lower strain rates the deformation is controlled by a combination of creep processes and plastic flow. In the range of high speed deformation the mechanical behaviour can be described with damping controlled gliding. So the complete strain rate range can be described as follows:

$$\dot{\varepsilon} = (1-M)\left(\left(\frac{\sigma}{\sigma_0(T,\varepsilon)}\right)^{N(T)} + \left(\frac{\sigma}{\sigma_H(T,\varepsilon)}\right)^{\frac{1}{m(T)}}\right) + M\left(\frac{\sigma - \sigma_G(T,\varepsilon)}{\eta} + \dot{\varepsilon}_G\right) \tag{3}$$

where $M = (T, \varepsilon, \dot{\varepsilon})$ is a transition function between dynamic strain rates and lower strain rates. The stress and strain rate for the transition point is given by:

$$\sigma_G(T,\varepsilon) = \sigma_H(T,\varepsilon)\dot{\varepsilon}_G^{\,m(T)} \text{ and } \dot{\varepsilon}_G = \left(m(T)\cdot\sigma_H(T,\varepsilon)/\eta\right)^{\frac{1}{(1-m(T))}} \quad (4)$$

With fitted values for the parameters $\sigma_0(T,\varepsilon)$, $\sigma_H(T,\varepsilon)$, $m(T)$, and $N(T)$ the full range of strain rates and temperatures can be described (Figure 6).

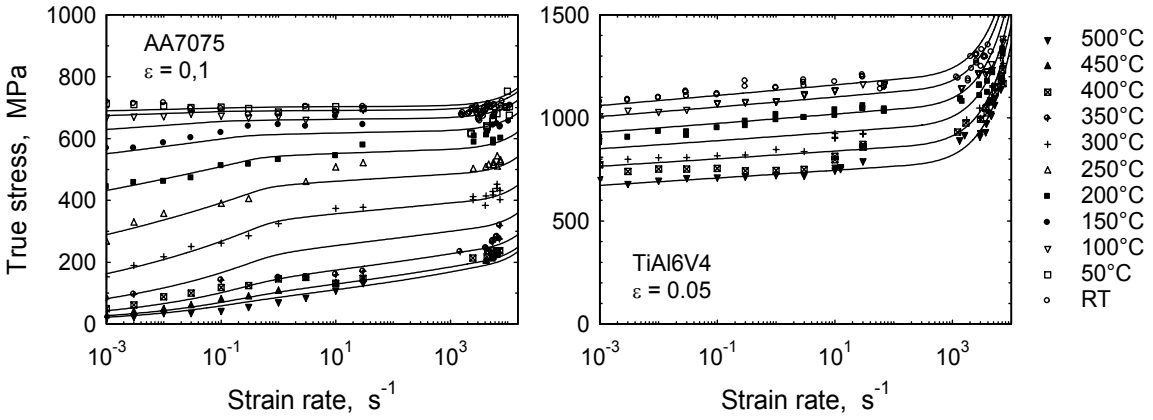

Figure 6: *Description of the material behaviour of AA7075 and Ti-6Al-4V in a wide range of strain rate and temperature [8]*

4 Computational results

4.1 Simulation of compression and shear tests

Compression and shear tests on the investigated materials at room temperature were simulated by the finite element method. The material behaviour in the quasi-static (ABAQUS\Standard, axisymmetrical), and the dynamic (ABAQUS\Explicit, axisymmetrical) simulations was described by the constitutive material law Equation (2). In both cases the numerical simulation was calculated up to the experimentally determined global deformation at fracture considering Coulomb friction with a coefficient μ=0.1. In Figure 7 the experimental and computation results at the fracture are plotted for the quasi-static isothermal ($\dot{\varepsilon}$ = 0,001 s^{-1}, Figure 7 a-d) and dynamic adiabatic ($\dot{\varepsilon}$ = 5010 s^{-1}, Figure 7 e-k) compression tests on AA7075. Under quasi-static loading the local distributions of the equivalent strain and stress have the same tendency and symmetry along the compression cones (Figure 7c, d). Oppositely, asymmetrical distribution (Figure 7g, k) was obtained in the dynamic case due to the effect of wave reflection from the output bar, which is consent with the experimental results shown in Figure 7f. The highest values of local plastic strain correspond to the lowest values of local stress (Figure 7g, k) due to decreasing of the adiabatic flow curve after reaching to maximum value as represented in Figure 7e. The ratio between maximum local deformation $\hat{\varepsilon}_{fr}$ and global deformation $\overline{\varepsilon}_{fr}$ reaches a value of 1.36 in case of quasi-static loading. In case of dynamic loading this ratio increases up to a value of 1.61 due to deformation localisation in the adiabatic shear bands.

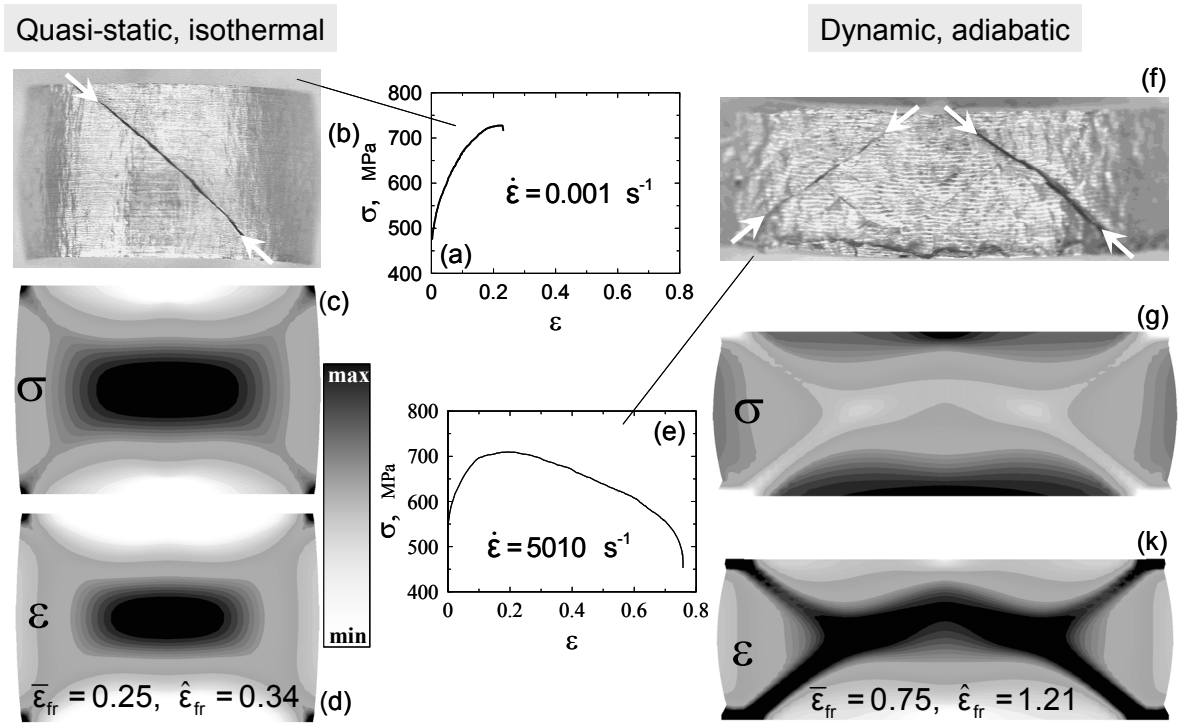

Figure 7: *Experimental and simulation results of compression test for quasi-static and dynamic loading on AA7075*

Figure 8 represents optical micrograph (Longitudinal sections) of hat shaped specimens of AZ80 deformed up to the fracture under quasi-static ($\dot{\gamma} = 0.0173\,s^{-1}, \vartheta = 20°C$) and impact ($\dot{\gamma} = 116000\,s^{-1}, \vartheta = 20°C$) loading as well as the results of its numerical simulations (local shear stress and shear strain distributions). In both cases the investigated specimens come to ductile shear fracture, whereby shear localisation was observed by dynamic loading, Figure 8f. In quasi-static simulation, the failure zone of the specimen exhibits relatively diffuse shear strain distribution and does not appear to localise, Figure 8d. Oppositely, by dynamic loading the deformation is localised due to thermal softening of the material and higher values of shear strain are reached (Figure 8h), which is in agreement with the experimental results.

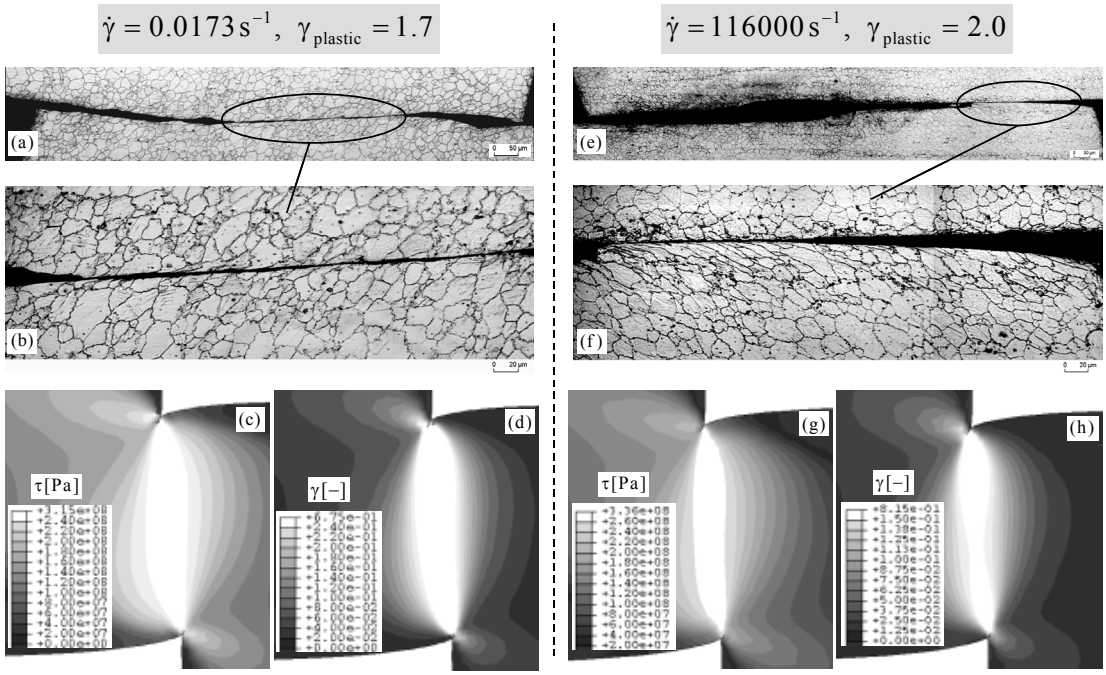

Figure 8: *Shear strain localization by impact shear test on AZ80 (ϑ = 20°C)*

4.2 Failure criterion for ductile fracture

Figure 9 shows the results of the FE-Simulations of smooth tensile specimens and differently notched bars of Al-alloy AA7075 T7351.

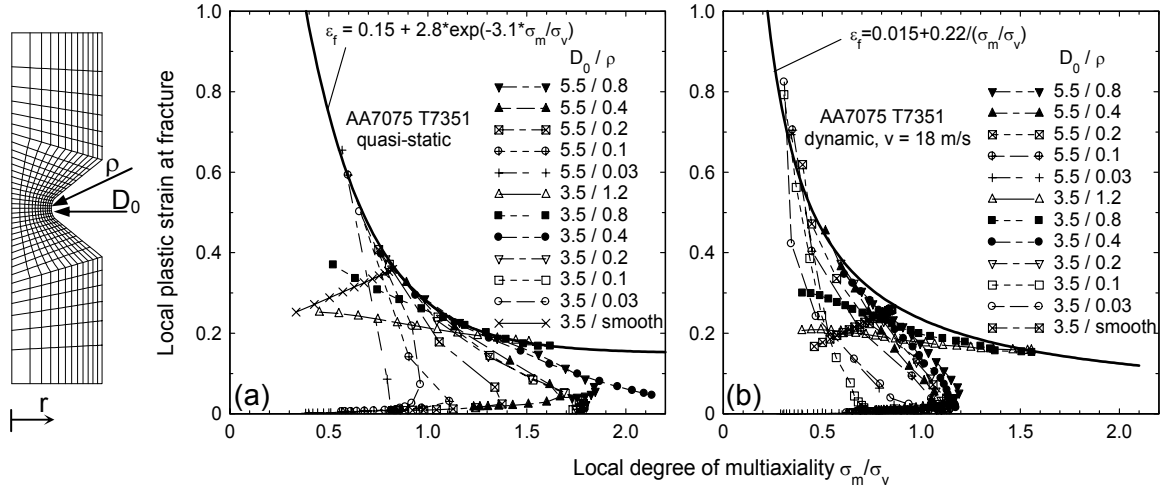

Figure 9: *Local equivalent plastic strain at fracture as a function of the degree of multiaxiality (σ_m/σ_v) along the specimen radius at the narrowest cross-section of differently notched specimen of aluminium AA7075 T7351 under (a) quasi-static (ABAQUS/Standard) and (b) dynamic loading (ABAQUS/Explicit) [9]*

The failure criterion for AA7075 was defined by the local failure strain $\bar{\varepsilon}_f$ as a function of the ratio between local mean stress σ_m and local equivalent stress σ_v. Such a criterion was deduced considering that ductile fracture occurs due to nucleation, growth, and coalescence of micro-cavities. The experimental specimen elongation at fracture was used as

a termination time point for the FE-Simulation. The corresponding values of the local equivalent plastic strain $\bar{\varepsilon}(r)$ and degree of multiaxiality were computed for the different notch geometries at the different Gauss-integration points along the radius r of the specimen in the narrowest cross-section D_0. The results are represented by a continuous curve for each geometry. Each point of the curve represents a location r along the radius in the smallest cross-section. Only one point of each curve fulfils the failure criterion, so that the envelope of all curves represents the failure criterion. For quasi-static loading, the envelope is described by the Hancock/Mackenzie relation [10], and for dynamic loading by [11]. Under quasi-static loading, the local effective plastic strain for a given degree of multiaxiality is higher than in the case of dynamic loading.

5 Conclusions

- The mechanical behaviour of materials at high strain rates is mainly characterised by increased strain rate sensitivity and the adiabatic character of the deformation process
- Under impact loading the ductility of AA7075 and AZ80 increases sharply with strain rate due to the higher strain rate sensitivity, while it decreases for Ti-6Al-4V due to the dominating rate dependence of the damage process
- Deformation localisation and shear band cause the damage in AA7075, AZ80, and Ti-6Al-4V under dynamic compression loading
- The mechanical flow behaviour of the investigated alloys was characterised with adequate constitutive material laws
- In order to validate the used constitutive material laws, compression, tension and shear tests were simulated by the finite element method.

References

[1] *Lips, H.; Brodmann, M.; El-Magd, E.*: J. Phys. IV 10 (2000) 371.
[2] *Neubauer, A.; Stroppe, H.; Wolf, H.*: Verlag Technik, Berlin 1988.
[3] *El-Magd, E.; Treppmann, C.; Weisshaupt, H.*: J. Phys. IV, suppl. III, 1997, 511.
[4] *Lippmann, H.*: Springer Verlag, Berlin, 1981, 210.
[5] *Sakino, K.; Shiori, J.*: J. Physique. IV, suppl. III, 1991, 1, C3.
[6] *El-Magd, E.*: J. Phys. IV, suppl. J. Phys. III 1994, 4, 149.
[7] *Taylor, G.I.; Quinney, H.*: Proc. R. Soc. A413 (1934) 307.
[8] *Treppmann, C.*: PhD-Thesis, RWTH Aachen, Germany, 2001.
[9] *Brodmann, M.*: PhD-Thesis, RWTH Aachen, Germany, 2001.
[10] *Hancock, J.W.; Mackenzie, A.Z.*: J. Mech. Phys. Solids 24 1976, 147.
[11] *El-Magd, E.*: Steel Res. 68 2 1997, 67.